ACS APPLIED POLYMER MATERIALS

pubs.acs.org/acsapm Article

Supramolecular Assembly Based on Sulfato-β-cyclodextrin for Hypoxia Cell Imaging

Hui-Juan Wang, Heng-Yi Zhang, Cong Zhang, Bing Zhang, Xianyin Dai, Xiufang Xu, and Yu Liu*

Cite This: ACS Appl. Polym. Mater. 2022, 4, 2935−2940 Read Online

ACCESS | Metrics & More | Article Recommendations | Supporting Information

ABSTRACT: Constructing hypoxia fluorescence probes is a developing research field, due to the hypoxic nature of many diseases, caused by an inadequate supply of oxygen. Herein, we reported a noncovalent hypoxia-responsive turn-on fluorescence probe, constructed by biocompatible sulfato-β-cyclodextrin (SCD), azobenzene derivative (**1**), and fluorochrome rhodamine 123 (Rho123). TEM image and dynamic light scattering (DLS) indicated that negatively multicharged SCD and positively charged **1** aggregated into nanoparticles with an average diameter of 53.8 nm through electrostatic interactions. The critical aggregation concentration (CAC) of **1** in the presence of SCD was obtained as 0.028 mM investigated by optical transmittance experiments quantitatively. The supramolecular assembly (SCD/**1**) works as both carrier and fluorescent quencher of Rho123. Verified by UV/vis absorption experiments, the azobenzene derivative **1** can be reduced efficiently by chemical reductant with a rate constant of 1.598 min^{-1}. Florescence experiments showed that SCD/**1** made a thoroughly quenching of Rho123 and 8-fold recovery of fluorescence intensity after reduced. Under hypoxia condition the azobenzene group of **1** was reduced by azo reductase, accompanying with the release and fluorescence recovery of Rho123. The noncovalent hypoxia-responsive ternary supramolecular assembly was used for hypoxia cell imaging.

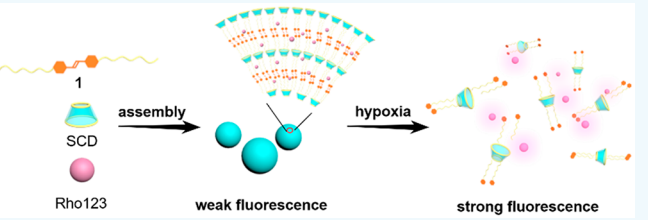

KEYWORDS: *hypoxia, azobenzene, sulfato-β-cyclodextrin, PET, cell imaging*

INTRODUCTION

Hypoxia is an important indicator of solid tumor caused by the rapidly proliferating and expanding of neoplasms, insufficient oxygen supply, and hindered oxygen diffusion by poor adapted vascularization.[1,2] Therefore, the research on hypoxia-responsive probes is essential for the diagnosis and treatment of various diseases.[3−5] The high expression level of various bioreductive enzymes in solid tumor due to the low concentration of oxygen results in an enhanced reductive stress microenvironment.[6,7] Many hypoxic-sensitive groups such as azo,[8,9] nitroimidazole,[10−12] quinones,[13] and *N*-oxides,[14−16] which were all reducible compounds,[17,18] were introduced into probes and used in many fields, such as tumor hypoxia detecting,[19] fluorescence imaging,[20,21] drug delivery,[16,22−25] and so on. Among them, azo derivatives as old and extensively studied compounds, possessing the character of reversible photoisomerization and being redox-responsive, have been widely used in biological systems in recent years.[26] The fluorescence of chromophores can be quenched by azo due to the quick dissipation of excited state energies caused by a rapid conformation transition of the N═N bond.[27] Interestingly, the restoration of fluorescence can be realized after the reduction of the N═N bond in an azo derivative under reducing conditions (such as hypoxia, in the presence of chemical reductant or bioreductase). In recent years, many hypoxia imaging probes derived from the azo group were reported.[28] Nagano *et al.* reported a hypoxia-responsive near-infrared fluorescent probe used for hypoxia imaging and real-time monitoring of ischemia, which is the first hypoxia probe with the azo group as a quencher.[29] Subsequently, they directly conjugated the azo group to fluorescent rhodamine derivatives and got two probes with different hypoxia detection thresholds.[30] Zhu *et al.* constructed a novel probe for hypoxia imaging by conjugated azonaphthalimide and rhodamine B.[19] He *et al.* reported a reversible azo-conjugated fluorescent probe and used it for cycling hypoxia imaging.[31] As far as we know, most of them are constructed through a covalent method by linking the azo group to a fluorophore with high fluorescence yield. In 2019, Guo *et al.* constructed a hypoxia imaging probe through a noncovalent strategy based on a supramolecular host−guest interaction.[32] Supramolecular chemistry[33−35] provides an alternative method to design hypoxia imaging probes, which show easy synthesis, low toxicity, and flexibility. Herein, we constructed a hypoxia-responsive fluorescence probe through

Received: February 4, 2022
Accepted: March 9, 2022
Published: March 24, 2022

https://doi.org/10.1021/acsapm.2c00228
ACS Appl. Polym. Mater. 2022, 4, 2935−2940

Scheme 1. Schematic Illustration of a Hypoxia-Responsive System and Molecular Structures of SCD, 1 and Rho123

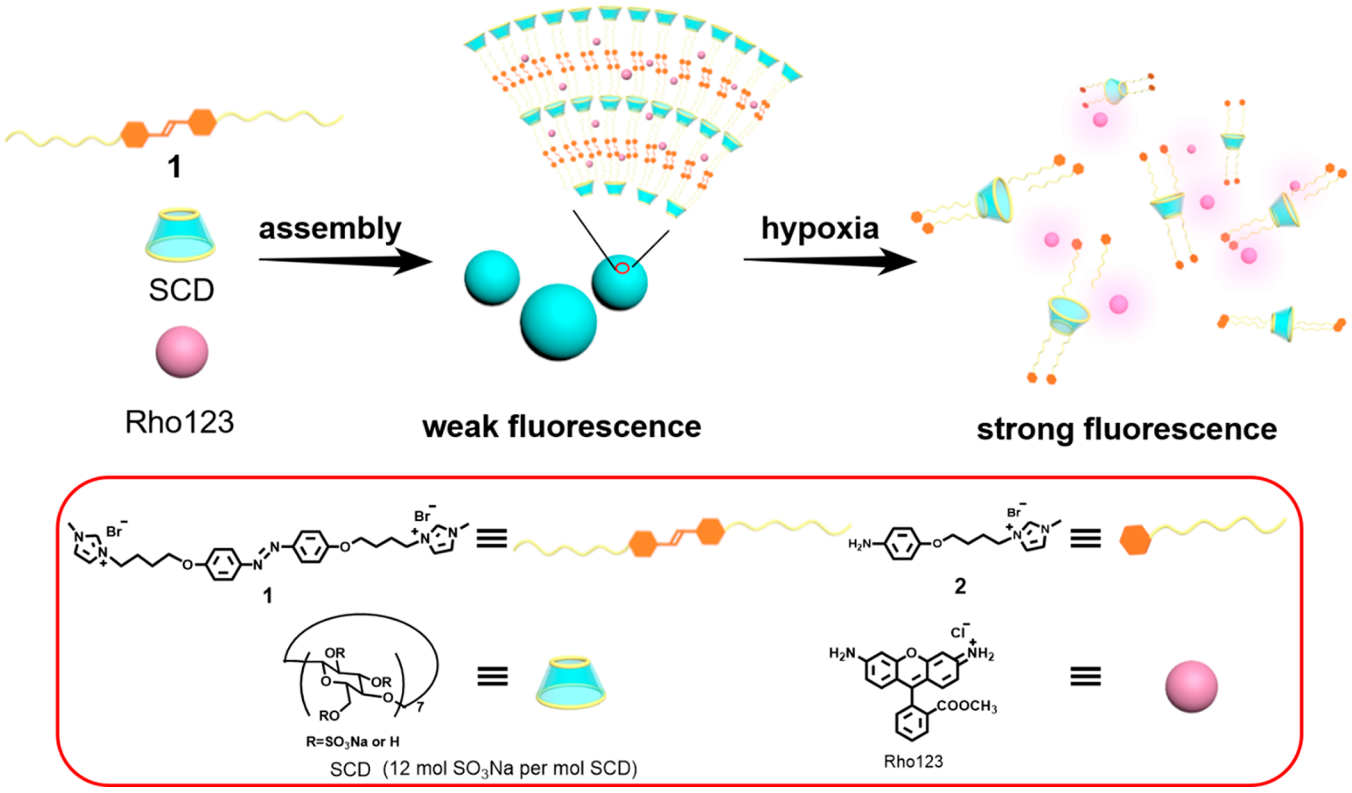

the electrostatic interactions of sulfato-β-cyclodextrin (SCD) and an azobenzene derivative (**1**). In this system, commercial dye rhodamine 123 (Rho123) was loaded and its fluorescence was quenched. Under hypoxic conditions, the azo group of **1** gets reduced, leading to the release of dyes and restoration of their fluorescence (Scheme 1).

RESULTS AND DISCUSSION

A water-soluble supramolecular assembly was constructed by SCD and azobenzene derivative **1** through electrostatic interactions. SCD was commercially available, and **1** was obtained in 81% yield through a simple synthetic route (Scheme S1). The ^{1}H NMR, ^{13}C NMR, and ESI-MS spectra of **1** are shown in the Supporting Information (Figure S1−S3). Molecule **1**, composed of cationic imidazole groups and hydrophobic alkyl chains, can form aggregates with SCD through electrostatic interactions. The aggregation behaviors of **1** in the presence of SCD were investigated by optical transmittance experiments quantitatively. In the presence of SCD, the optical transmittance of **1** decreased due to the formation of large aggregates (Figure 1a). And the critical aggregation concentration (CAC) of **1** in the presence of SCD was obtained as 0.028 mM by monitoring the dependence of the optical transmittance at 520 nm on the concentration of **1** (Figure 1b). While the optical transmittance experiments of **1** in the absence of SCD proceeded through the same method (Figure S5), no distinct changes in the optical transmittance at 520 nm were observed, indicating that **1** cannot form aggregates without SCD. Furthermore, the optical transmittance of **1** at a fixed concentration (1.2×10^{-4} M) with addition of different concentrations of SCD was monitored (Figure 1c). With the increase of the concentration of SCD, the optical transmittance of the SCD/**1** solution at 520 nm

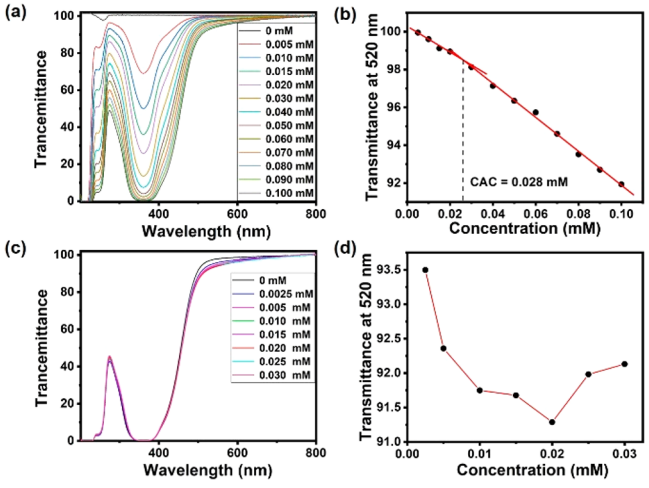

Figure 1. (a) Optical transmittance of SCD (2×10^{-5} M) with different concentrations of **1** in PBS buffer at 298 K. (b) Dependence of the optical transmittance at 520 nm on the concentration of **1** in the presence of SCD (2×10^{-5} M) in PBS buffer at 298 K. (c) Optical transmittance of **1** (1.2×10^{-4} M) with different concentrations of SCD in water at 298 K. (d) Dependence of the optical transmittance at 520 nm on the concentration of SCD in the presence of **1** (1.2×10^{-4} M) in PBS buffer at 298 K.

decreased and then increased with a minimum at a SCD concentration of 2×10^{-5} M (Figure 1d), indicating that the best molar ratio for SCD/**1** was 1:6. Subsequently, the aggregation behaviors of **1** in the presence of SCD were quantitatively investigated by dynamic light scattering (DLS), ζ potential, and transmission electron microscopy (TEM). As shown in Figure 2a, the SCD/**1** assembly showed an average diameter of 53.83 nm. The TEM image indicated that

https://doi.org/10.1021/acsapm.2c00228
ACS Appl. Polym. Mater. 2022, 4, 2935−2940

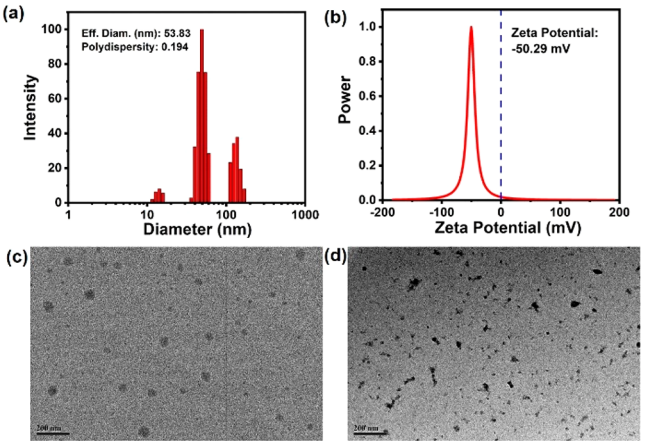

Figure 2. (a) DLS data and (b) ζ potential and TEM of SCD/**1** (c) before and (d) after adding SHS (scale bar: 200 nm).

numerous uniform nanoparticles were formed by an SCD/**1** aggregate (Figure 2c). The particles showed negative ζ potential (−50.29 mV), indicating that the surface of the nanoparticles was negative charged (Figure 2b). The SCD is composed of randomly sulfonated cyclodextrins with an average degree of substitution of 12. The negative ζ potential is mainly due to the negative charges on SCD upon aggregation with **1**. Furthermore, the UV/vis experiments of SCD/**1** with different concentrations of Rho123 were executed. As shown in Figure S8c, no obvious change about the absorption peak of SCD/**1** was observed, indicating the addition of Rho123 did not affect the assembly of SCD/**1**. Combining with the hydrophilic and hydrophobic properties, it is reasonable to speculated SCD/**1** form nanoparticles through layers of stacked.[36]

Furthermore, the reducible capacity of SCD/**1** was examined by UV/vis spectroscopy. As reported azobenzene derivatives,[37] **1** showed a strong $\pi-\pi^*$ transition band at 360 nm and a weak $n-\pi^*$ transition band around 400 nm (Figure 3a, red line).

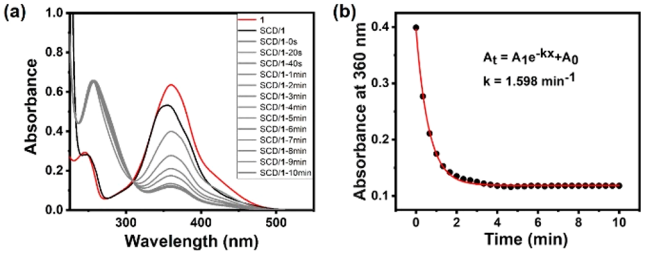

Figure 3. (a) Absorbance spectra of **1** (24 μM), SCD/**1** (4 μM/24 μM) at different time after the addition of SHS. (b) Absorbance of SCD/**1** (4 μM/24 μM) at 360 nm as a function of time following addition of SHS in PBS buffer and the corresponding curve according to the quasi-first-reaction decay model.

After adding SCD into the solution of **1**, the absorption of **1** changes with blue shift (Figure 3a, black line), owing to the formation of aggregation. Upon addition of excess sodium hydrogen sulfite (SHS), a chemical reductant to mimic azoreductase, the color of SCD/**1** changed from yellow to colorless transparent within 5 min (photos in Figure 3a). The reducing kinetics were calculated according to the real time absorbance at 360 nm. The curve of the absorbance at 360 nm depending on time was well fitted in a quasi-first-order reaction decay model (adjusted $R^2 > 0.998$), giving the rate constant 1.598 min^{-1} (Figure 3b). The half-life was calculated as 25.6 s. The mass spectrometry analysis was used to examine the reduction product of **1**. The ESI-MS spectrum of **1** showed peaks at 244.1447 and 244.6469, which are corresponding to $[M - 2Br^-]^{2+}$ (Figure S3). After adding chemical reductant SHS, compound **1** was reduced and produced phenylamine derivatives **2**, evidenced by the appearance of peaks at 246.16039 and 247.16410 in the ESI-MS spectrum corresponding to $[M - Br^-]^+$ (Figure S4). Besides the use of a chemical reductant, **1** could also be reduced by bioreductase. Next, the nicotinamide adenine dinucleotide phosphate (NADPH) in the presence of DT-diaphorase, a reductase which was overexpressed in many cancers and can be activated under hypoxia, were added to SCD/**1** solution.[38] In normoxia condition, there were no changes in the absorbance of SCD/**1** (Figure S7a). After putting the solution under hypoxia conditions for several minutes, the absorbance of SCD/**1** around 360 nm decreased similar to the addition of SHS, which means the azo bond was successfully reduced under hypoxia conditions (Figure S7b).[39,40] All these results confirmed that SCD/**1** showed good reducibility to both chemical reductant and bioreductase, making the fluorescence restore of commercial dyes possible.

Furthermore, we explored the reducibility of SCD/**1** through fluorescence after loading Rho123. As shown in Figure S8a, the fluorescence intensity of Rho123 decreased and reached the lowest value (I_{free}/I_{load} = 13) upon the gradual addition of 4 equiv of SCD/**1**. It is very important to explore the fluorescence quenching mechanism in the noncovalent hypoxia imaging system. Currently, most of the hypoxia imaging probes are covalent systems and are based on the fluorescence quenching mechanism of ultrafast photoinduced isomerization of azo groups or Förster resonance energy transfer (FRET).[19,29,30,41] Due to the noncovalent interaction other than covalent conjugation between SCD/**1** and Rho123, it is impossible that the fluorescence quenching of Rho123 was caused by the fast conformation change of azobenzene.[30,42] As shown in Figure S6, there was no appreciable overlap between the absorption spectrum of SCD/**1** and the fluorescence emission spectrum of Rho123, excluding the FRET quenching mechanism. We speculated that the fluorescence quenching of Rho123 may be caused by **1** through the photoinduced electron transfer (PET) mechanism.[43] Simple molecular orbital theory is a common tool used to discuss fluorescence switching problems.[44] According to the calculation results, the HOMO and LUMO energy of Rho123 is lower than the HOMO and LUMO energy of compound **1**, respectively, which leads to the emergence of a reducing PET process. As shown in Figure 4, the HOMO−LUMO orbital energy difference of the fluorescent molecule Rho123 is 3.07 eV. After the electrons of fluorescent molecule Rho123 are excited, it is difficult to return to its HOMO orbital. Because the HOMO orbital energy of Rho123 is lower than the HOMO orbital energy of compound **1** by 0.13 eV, and electrons from the HOMO orbital of compound **1** are more easily transferred to the HOMO orbital of Rho123, occupying the HOMO orbital of Rho123 and quenching the fluorescence. Furthermore, **Azo−OH** (Scheme S2) as one of the building units of **1** was explored as a reference. The **Azo−OH** showed higher HOMO energy than Rho123 (Table S1), but only slight quenching of fluorescence was caused by adding **Azo−OH** into the solution of Rho123 (Figure S9). All in all, it is rational to believe that

https://doi.org/10.1021/acsapm.2c00228
ACS Appl. Polym. Mater. 2022, 4, 2935−2940

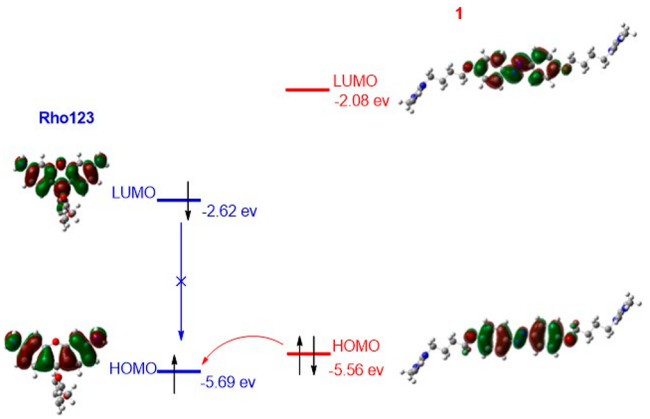

Figure 4. Frontier orbital energy diagrams and the electron-transfer path from **1** to Rho123.

the fluorescence quenching of Rho123 was caused by **1** through the photoinduced electron transfer (PET) mechanism.

As expected, the fluorescence intensity of Rho123 was gradually increased and reached 8-fold of the original intensity with the break of azobenzene in **1** after adding SHS to the solution (Figure 5a). Such an apparent increasing of

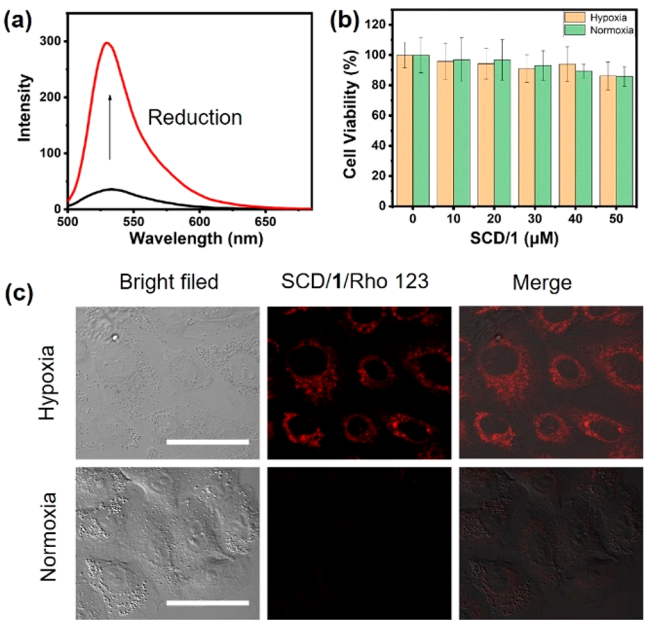

Figure 5. (a) Fluorescence spectra of SCD/**1**/Rho123 (20 μM/120 μM/5 μM) before and after reducing by SHS. (b) Viabilities of A549 cells upon incubation with different concentrations of SCD/**1** (from 0 μM/0 μM to 50 μM/300 μM) under hypoxia and normoxia conditions, respectively. The error bars represent ±sem (n = 4 independent experiments). (c) Confocal laser scanning microscopy images of A549 cells incubated with SCD/**1**/Rho123 (20 μM/120 μM/5 μM) under hypoxia (less than 0.1% O_2) or normoxia (20% O_2) conditions for 10 h. The Rho123 emission was obtained using excitation at 488 nm. Scale bar: 20 μm.

fluorescence intensity indicated the feasibility of the non-covalent assembly in hypoxia imaging. The operating principle is based on the fracture of the N═N bond in **1** accompanying the disassembly of SCD/**1** under hypoxia conditions. No significant changes in the fluorescence intensity of SCD/**1**/Rho123 were observed when adding biological species (cysteine, homocysteine, glutathione, and NADPH), indicating that the strong binding of the ternary assembly can resist the interference of many biological species (Figure S10).

After exploring the *in vitro* fluorescence off-on response of SCD/**1**/Rho123, we investigated their application in hypoxia-selective imaging in living cells. Furthermore, the A549 cells were incubated for 10 h under hypoxia and normoxia conditions after addition of SCD/**1**/Rho123. Then the cells were washed with phosphate buffer for 3 times and imaged by laser confocal microscopy. As shown in Figure 5, the A549 cells coincubated with the ternary supramolecular assembly SCD/**1**/Rho123 under hypoxia condition showed bright fluorescence, while the fluorescence of cells incubated under normoxia condition was negligible. These results proved that the SCD/**1**/Rho123 system show good fluorescence off-on response to oxygen. The cytotoxicity of SCD/**1** was evaluated by a cell counting kit-8 (CCK-8) assay with various concentrations of SCD/**1** from 0 μM/0 μM to 50 μM/300 μM, under hypoxic and normoxic conditions for 12 h. The results of cell cytotoxicity experiments showed that the SCD/**1** had negligible cytotoxicity.

CONCLUSION

In summary, a hypoxia-responsive fluorescence turn-on system for activatable cell imaging was constructed based on a facile supramolecular strategy. In this system, the easily obtained **1** can aggregated to form supramolecular nanoparticles with an average diameter of 53.8 nm induced by commercially obtained SCD. The CAC of SCD/**1** was measured as 0.028 mM by optical transmittance experiments quantitatively. Furthermore, the supramolecular assembly was used as a carrier of fluorochrome Rho 123 and showed excellent fluorescence quenching effect to Rho123 (I_{free}/I_{load} = 13). The quantum chemical calculation indicated that the quenching mechanism was PET. The UV/vis experiments indicated that the azobenzene derivative can be reduced by both chemical and biological reductant efficiently. The fluorescence intensity of Rho 123 restored 8-fold after adding chemical reductant to the ternary supramolecular assembly. Benefiting from the hypoxia-responsive fluorescence character, the ternary supramolecular assembly was used for hypoxia imaging of A549 cells.

ASSOCIATED CONTENT

Supporting Information

The Supporting Information is available free of charge at https://pubs.acs.org/doi/10.1021/acsapm.2c00228.

Detailed synthetic procedure, ^{1}H NMR, ^{13}C NMR, and HRMS spectra of **1**, UV−vis absorbance experiments, fluorescence experiments, and theoretical calculations (PDF)

AUTHOR INFORMATION

Corresponding Author

Yu Liu − *Department of Chemistry, State Key Laboratory of Elemento-Organic Chemistry, Nankai University, Tianjin 300071, P. R. China;* orcid.org/0000-0001-8723-1896; Email: yuliu@nankai.edu.cn

https://doi.org/10.1021/acsapm.2c00228
ACS Appl. Polym. Mater. 2022, 4, 2935−2940

Authors

Hui-Juan Wang − *Department of Chemistry, State Key Laboratory of Elemento-Organic Chemistry, Nankai University, Tianjin 300071, P. R. China*

Heng-Yi Zhang − *Department of Chemistry, State Key Laboratory of Elemento-Organic Chemistry, Nankai University, Tianjin 300071, P. R. China*

Cong Zhang − *Department of Chemistry, State Key Laboratory of Elemento-Organic Chemistry, Nankai University, Tianjin 300071, P. R. China*

Bing Zhang − *Department of Biochemistry and Molecular Biology, Key Laboratory of Immune Microenvironment and Disease (Ministry of Education), School of Basic Medical Sciences, Tianjin Medical University, Tianjin 300070, P. R. China*

Xianyin Dai − *Department of Chemistry, State Key Laboratory of Elemento-Organic Chemistry, Nankai University, Tianjin 300071, P. R. China*

Xiufang Xu − *Department of Chemistry, State Key Laboratory of Elemento-Organic Chemistry, Nankai University, Tianjin 300071, P. R. China;* orcid.org/0000-0002-3510-3267

Complete contact information is available at: https://pubs.acs.org/10.1021/acsapm.2c00228

Notes

The authors declare no competing financial interest.

■ ACKNOWLEDGMENTS

We thank the National Natural Science Foundation of China (21861132001, 21772099, and 21772100) for financial support.

■ ABBREVIATIONS

SCD, sulfato-β-CD; Rho 123, rhodamine 123; SHS, sodium hydrogen sulfite

■ REFERENCES

(1) Han, J.; Won, M.; Kim, J. H.; Jung, E.; Min, K.; Jangili, P.; Kim, J. S. Cancer stem cell-targeted bio-imaging and chemotherapeutic perspective. *Chem. Soc. Rev.* **2020**, *49*, 7856−7878.

(2) Liu, Z.; Xue, Y.; Wu, M.; Yang, G.; Lan, M.; Zhang, W. Sensitization of Hypoxic Tumor to Photodynamic Therapy via Oxygen Self-Supply of Fluorinated Photosensitizers. *Biomacromolecules.* **2019**, *20*, 4563−4573.

(3) Lv, Z.; Zou, L.; Wei, H.; Liu, S.; Huang, W.; Zhao, Q. Phosphorescent Starburst Pt(II) Porphyrins as Bifunctional Therapeutic Agents for Tumor Hypoxia Imaging and Photodynamic Therapy. *ACS Appl. Mater. Interfaces.* **2018**, *10*, 19523−19533.

(4) Feng, Z.; Tao, P.; Zou, L.; Gao, P.; Liu, Y.; Liu, X.; Wang, H.; Liu, S.; Dong, Q.; Li, J.; Xu, B.; Huang, W.; Wong, W.-Y.; Zhao, Q. Hyperbranched Phosphorescent Conjugated Polymer Dots with Iridium(III) Complex as the Core for Hypoxia Imaging and Photodynamic Therapy. *ACS Appl. Mater. Interfaces.* **2017**, *9*, 28319−28330.

(5) An, L.; Wang, Y.; Lin, J.; Tian, Q.; Xie, Y.; Hu, J.; Yang, S. Macrophages-Mediated Delivery of Small Gold Nanorods for Tumor Hypoxia Photoacoustic Imaging and Enhanced Photothermal Therapy. *ACS Appl. Mater. Interfaces.* **2019**, *11*, 15251−15261.

(6) Kizaka-Kondoh, S.; Inoue, M.; Harada, H.; Hiraoka, M. Tumor hypoxia: A target for selective cancer therapy. *Cancer. Sci.* **2003**, *94*, 1021−1028.

(7) Shen, Y.; Zhang, Q.; Qian, X.; Yang, Y. Practical Assay for Nitrite and Nitrosothiol as an Alternative to the Griess Assay or the 2,3-Diaminonaphthalene Assay. *Anal. Chem.* **2015**, *87*, 1274−1280.

(8) Liu, X.; Meng, C.; Ji, G.; Liu, J.; Zhu, P.; Qian, J.; Zhu, S.-X.; Zhang, Y.; Ling, Y. Tumor microenvironment-activatable boolean logic supramolecular nanotheranostics based on a pillar[6]arene for tumor hypoxia imaging and multimodal synergistic therapy. *Mater. Chem. Front.* **2021**, *5*, 5846−5856.

(9) Wu, Y.; Zhang, H.-Y.; Liu, Y. Application of Azobenzene Derivative Probes in Hypoxia Cell Imaging. *Prog. Chem.* **2021**, *33*, 331−340.

(10) Brennecke, B.; Wang, Q.; Zhang, Q.; Hu, H.-Y.; Nazaré, M. An Activatable Lanthanide Luminescent Probe for Time-Gated Detection of Nitroreductase in Live Bacteria. *Angew. Chem., Int. Ed.* **2020**, *59*, 8512−8516.

(11) Wang, L.; Wang, H.; Shen, K.; Park, H.; Zhang, T.; Wu, X.; Hu, M.; Yuan, H.; Chen, Y.; Wu, Z.; Wang, Q.; Li, Z. Development of Novel 18F-PET Agents for Tumor Hypoxia Imaging. *J. Med. Chem.* **2021**, *64*, 5593−5602.

(12) Hoigebazar, L.; Jeong, J. M.; Lee, J.-Y.; Shetty, D.; Yang, B. Y.; Lee, Y.-S.; Lee, D. S.; Chung, J.-K.; Lee, M. C. Syntheses of 2-Nitroimidazole Derivatives Conjugated with 1,4,7-Triazacyclononane-N,N-Diacetic Acid Labeled with F-18 Using an Aluminum Complex Method for Hypoxia Imaging. *J. Med. Chem.* **2012**, *55*, 3155−3162.

(13) Komatsu, H.; Shindo, Y.; Oka, K.; Hill, J. P.; Ariga, K. Ubiquinone-Rhodol (UQ-Rh) for Fluorescence Imaging of NAD(P)H through Intracellular Activation. *Angew. Chem., Int. Ed.* **2014**, *53*, 3993−3995.

(14) Xu, C.; Zou, H.; Zhao, Z.; Zhang, P.; Kwok, R. T. K.; Lam, J. W. Y.; Sung, H. H. Y.; Williams, I. D.; Tang, B. Z. A New Strategy toward "Simple" Water-Soluble AIE Probes for Hypoxia Detection. *Adv. Funct. Mater.* **2019**, *29*, 1903278.

(15) Liu, Z.; Song, F.; Shi, W.; Gurzadyan, G.; Yin, H.; Song, B.; Liang, R.; Peng, X. Nitroreductase-Activatable Theranostic Molecules with High PDT Efficiency under Mild Hypoxia Based on a TADF Fluorescein Derivative. *ACS Appl. Mater. Interfaces.* **2019**, *11*, 15426−15435.

(16) Karan, S.; Cho, M. Y.; Lee, H.; Lee, H.; Park, H. S.; Sundararajan, M.; Sessler, J. L.; Hong, K. S. Near-Infrared Fluorescent Probe Activated by Nitroreductase for In Vitro and In Vivo Hypoxic Tumor Detection. *J. Med. Chem.* **2021**, *64*, 2971−2981.

(17) Liu, J.-n.; Bu, W.; Shi, J. Chemical Design and Synthesis of Functionalized Probes for Imaging and Treating Tumor Hypoxia. *Chem. Rev.* **2017**, *117*, 6160−6224.

(18) Xue, T.; Shen, J.; Shao, K.; Wang, W.; Wu, B.; He, Y. Strategies for Tumor Hypoxia Imaging Based on Aggregation-Induced Emission Fluorogens. *Chem. Eur. J.* **2020**, *26*, 2521−2528.

(19) Cai, Q.; Yu, T.; Zhu, W.; Xu, Y.; Qian, X. A turn-on fluorescent probe for tumor hypoxia imaging in living cells. *Chem. Commun.* **2015**, *51*, 14739−14741.

(20) Xue, T.; Shao, K.; Xiang, J.; Pan, X.; Zhu, Z.; He, Y. In situ construction of a self-assembled AIE probe for tumor hypoxia imaging. *Nanoscale.* **2020**, *12*, 7509−7513.

(21) Kumari, R.; Sunil, D.; Ningthoujam, R. S. Naphthalimides in fluorescent imaging of tumor hypoxia - An up-to-date review. *Bioorg. Chem.* **2019**, *88*, 102979.

(22) Yuan, X.; Wang, Z.; Li, L.; Yu, J.; Wang, Y.; Li, H.; Zhang, J.; Zhang, Z.; Zhou, N.; Zhu, X. Novel fluorescent amphiphilic copolymer probes containing azo-tetraphenylethylene bridges for azoreductase-triggered release. *Mater. Chem. Front.* **2019**, *3*, 1097−1104.

(23) Kulkarni, P.; Haldar, M. K.; You, S.; Choi, Y.; Mallik, S. Hypoxia-Responsive Polymersomes for Drug Delivery to Hypoxic Pancreatic Cancer Cells. *Biomacromolecules.* **2016**, *17*, 2507−2513.

(24) Sharma, A.; Arambula, J. F.; Koo, S.; Kumar, R.; Singh, H.; Sessler, J. L.; Kim, J. S. Hypoxia-targeted drug delivery. *Chem. Soc. Rev.* **2019**, *48*, 771−813.

(25) Zhou, Y.; Ye, H.; Chen, Y.; Zhu, R.; Yin, L. Photoresponsive Drug/Gene Delivery Systems. *Biomacromolecules.* **2018**, *19*, 1840−1857.

(26) Beharry, A. A.; Woolley, G. A. Azobenzene photoswitches for biomolecules. *Chem. Soc. Rev.* **2011**, *40*, 4422−4437.

(27) Bandara, H. M. D.; Burdette, S. C. Photoisomerization in different classes of azobenzene. *Chem. Soc. Rev.* **2012**, *41*, 1809−1825.
(28) Kumari, R.; Sunil, D.; Ningthoujam, R. S.; Kumar, N. V. A. Azodyes as markers for tumor hypoxia imaging and therapy: An up-to-date review. *Chem. Bio. Interact.* **2019**, *307*, 91−104.
(29) Kiyose, K.; Hanaoka, K.; Oushiki, D.; Nakamura, T.; Kajimura, M.; Suematsu, M.; Nishimatsu, H.; Yamane, T.; Terai, T.; Hirata, Y.; Nagano, T. Hypoxia-Sensitive Fluorescent Probes for in Vivo Real-Time Fluorescence Imaging of Acute Ischemia. *J. Am. Chem. Soc.* **2010**, *132*, 15846−15848.
(30) Piao, W.; Tsuda, S.; Tanaka, Y.; Maeda, S.; Liu, F.; Takahashi, S.; Kushida, Y.; Komatsu, T.; Ueno, T.; Terai, T.; Nakazawa, T.; Uchiyama, M.; Morokuma, K.; Nagano, T.; Hanaoka, K. Development of Azo-Based Fluorescent Probes to Detect Different Levels of Hypoxia. *Angew. Chem., Int. Ed.* **2013**, *52*, 13028−13032.
(31) Zhang, Y.; Zhao, W.; Chen, Y.; Yuan, H.; Fang, H.; Yao, S.; Zhang, C.; Xu, H.; Li, N.; Liu, Z.; Guo, Z.; Zhao, Q.; Liang, Y.; He, W. Rational construction of a reversible arylazo-based NIR probe for cycling hypoxia imaging in vivo. *Nat. Commun.* **2021**, *12*, 2772.
(32) Geng, W.-C.; Jia, S.; Zheng, Z.; Li, Z.; Ding, D.; Guo, D.-S. A Noncovalent Fluorescence Turn-on Strategy for Hypoxia Imaging. *Angew. Chem., Int. Ed.* **2019**, *58*, 2377−2381.
(33) Wang, Q.; Zhang, Q.; Zhang, Q.-W.; Li, X.; Zhao, C.-X.; Xu, T.-Y.; Qu, D.-H.; Tian, H. Color-tunable single-fluorophore supramolecular system with assembly-encoded emission. *Nat. Commun.* **2020**, *11* (1), 158.
(34) Wang, C.; Wang, S.; Yang, H.; Xiang, Y.; Wang, X.; Bao, C.; Zhu, L.; Tian, H.; Qu, D.-H. A Light-Operated Molecular Cable Car for Gated Ion Transport. *Angew. Chem., Int. Ed.* **2021**, *60* (27), 14836−14840.
(35) Zong, Z.; Zhang, Q.; Qiu, S.-H.; Wang, Q.; Zhao, C.; Zhao, C.-X.; Tian, H.; Qu, D.-H. Dynamic Timing Control over Multicolor Molecular Emission by Temporal Chemical Locking. *Angew. Chem., Int. Ed.* **2022**, *61*, No. e202116414.
(36) Li, J.-J.; Chen, Y.; Yu, J.; Cheng, N.; Liu, Y. A Supramolecular Artificial Light-Harvesting System with an Ultrahigh Antenna Effect. *Adv. Mater.* **2017**, *29*, 1701905.
(37) Wang, H.-J.; Zhang, H.-Y.; Wu, H.; Dai, X.-Y.; Li, P.-Y.; Liu, Y. Photocontrolled morphological conversion and chiral transfer of a snowflake-like supramolecular assembly based on azobenzene-bridged bis(dibenzo-24-crown-8) and a cholesterol derivative. *Chem. Commun.* **2019**, *55*, 4499−4502.
(38) Ma, D.; Huang, C.; Zheng, J.; Zhou, W.; Tang, J.; Chen, W.; Li, J.; Yang, R. Azoreductase-Responsive Nanoprobe for Hypoxia-Induced Mitophagy Imaging. *Anal. Chem.* **2019**, *91*, 1360−1367.
(39) Rao, J.; Khan, A. Enzyme Sensitive Synthetic Polymer Micelles Based on the Azobenzene Motif. *J. Am. Chem. Soc.* **2013**, *135*, 14056−14059.
(40) Rao, J.; Hottinger, C.; Khan, A. Enzyme-Triggered Cascade Reactions and Assembly of Abiotic Block Copolymers into Micellar Nanostructures. *J. Am. Chem. Soc.* **2014**, *136*, 5872−5875.
(41) Liu, J.; Ding, G.; Chen, S.; Xue, C.; Chen, M.; Wu, X.; Yuan, Q.; Zheng, J.; Yang, R. Multifunctional Programmable DNA Nanotrain for Activatable Hypoxia Imaging and Mitochondrion-Targeted Enhanced Photodynamic Therapy. *ACS Appl. Mater. Interfaces.* **2021**, *13*, 9681−9690.
(42) Chevalier, A.; Mercier, C.; Saurel, L.; Orenga, S.; Renard, P.-Y.; Romieu, A. The first latent green fluorophores for the detection of azoreductase activity in bacterial cultures. *Chem. Commun.* **2013**, *49*, 8815−8817.
(43) Ueno, T.; Urano, Y.; Setsukinai, K.-i.; Takakusa, H.; Kojima, H.; Kikuchi, K.; Ohkubo, K.; Fukuzumi, S.; Nagano, T. Rational Principles for Modulating Fluorescence Properties of Fluorescein. *J. Am. Chem. Soc.* **2004**, *126*, 14079−14085.
(44) de Silva, A. P.; Gunaratne, H. Q. N.; Gunnlaugsson, T.; Huxley, A. J. M.; McCoy, C. P.; Rademacher, J. T.; Rice, T. E. Signaling Recognition Events with Fluorescent Sensors and Switches. *Chem. Rev.* **1997**, *97*, 1515−1566.

https://doi.org/10.1021/acsapm.2c00228
ACS Appl. Polym. Mater. 2022, 4, 2935−2940